



Nanovesicles displaying functional linear and branched oligomannose self-assembled from sequence-defined Janus glycodendrimers

Qi Xiao^{a,b}, Martina Delbianco^c, Samuel E. Sherman^a, Aracelee M. Reveron Perez^a, Priya Bharate^c, Alonso Pardo-Vargas^c, Cesar Rodriguez-Emmenegger^{d,e}, Nina Yu Kostina^{d,e}, Khosrow Rahimi^{d,e}, Dominik Söder^{d,e}, Martin Möller^{d,e}, Michael L. Klein^{b,1}, Peter H. Seeberger^{c,f,1}, and Virgil Percec^{a,1}

^aRoy & Diana Vagelos Laboratories, Department of Chemistry, University of Pennsylvania, Philadelphia, PA 19104; ^bInstitute of Computational Molecular Science, Temple University, Philadelphia, PA 19122; ^cDepartment of Biomolecular Systems, Max Planck Institute of Colloids and Interfaces, 14476 Potsdam, Germany; ^dDWI – Leibniz Institute for Interactive Materials, 52074 Aachen, Germany; ^eInstitute of Technical and Macromolecular Chemistry, RWTH Aachen University, 52074 Aachen, Germany; and ^fInstitute of Chemistry and Biochemistry, Freie Universität Berlin, 14195 Berlin, Germany

Contributed by Michael L. Klein, April 14, 2020 (sent for review March 3, 2020; reviewed by Jessica R. Kramer and Ling Peng)

Cell surfaces are often decorated with glycoconjugates that contain linear and more complex symmetrically and asymmetrically branched carbohydrates essential for cellular recognition and communication processes. Mannose is one of the fundamental building blocks of glycans in many biological membranes. Moreover, oligomannoses are commonly found on the surface of pathogens such as bacteria and viruses as both glycolipids and glycoproteins. However, their mechanism of action is not well understood, even though this is of great potential interest for translational medicine. Sequence-defined amphiphilic Janus glycodendrimers containing simple mono- and disaccharides that mimic glycolipids are known to self-assemble into glycodendrimersomes, which in turn resemble the surface of a cell by encoding carbohydrate activity via supramolecular multivalency. The synthetic challenge of preparing Janus glycodendrimers containing more complex linear and branched glycans has so far prevented access to more realistic cell mimics. However, the present work reports the use of an isothiocyanate-amine “click”-like reaction between isothiocyanate-containing sequence-defined amphiphilic Janus dendrimers and either linear or branched oligosaccharides containing up to six monosaccharide units attached to a hydrophobic amino-pentyl linker, a construct not expected to assemble into glycodendrimersomes. Unexpectedly, these oligoMan-containing dendrimers, which have their hydrophobic linker connected via a thiourea group to the amphiphilic part of Janus glycodendrimers, self-organize into nanoscale glycodendrimersomes. Specifically, the mannose-binding lectins that best agglutinate glycodendrimersomes are those displaying hexamannose. Lamellar “raft-like” nanomorphologies on the surface of glycodendrimersomes, self-organized from these sequence-defined glycans, endow these membrane mimics with high biological activity.

cell membrane mimics | isothiocyanate-amine coupling | automated glycan assembly

Cell membranes consist of phospholipids, glycolipids, cholesterol, and other components such as membrane proteins. There is much interest in developing synthetic analogs and models of these membrane components. To this end, synthetic lipids (1–5), amphiphilic block copolymers (6, 7), and Janus dendrimers (JDs) (8–10), have all been shown to self-assemble into nanoscale vesicles that mimic biological membranes. These vesicles are denoted as liposomes, polymersomes, and dendrimersomes (DSs), respectively. Synthetic amphiphilic JDs, constructed by orthogonal coupling of hydrophobic and hydrophilic dendrons, mimic phospholipids and self-assemble into stable DSs in water, buffer, and serum (8–13). DSs have a membrane thickness similar to phospholipids (~4 nm) (9, 10), which facilitated the development of hybrid vesicles from JDs with both bacteria and human cell membranes to transplant the

components of the natural membranes into the membranes of the hybrid synthetic cells (11, 12). DSs are very efficient for the encapsulation of hydrophobic organic molecules, including dyes and proteins (13). More recently, Janus glycodendrimers (JGDs) (14), the sugar-conjugated analogs of JDs, were designed to mimic glycolipids. JGDs containing mannose (Man) (14–16), galactose (Gal) (14, 15), lactose disaccharide (Lac) (14, 15, 17, 18), sulfated lactose (suLac) (19) and *N*-acetyl protected lactose derivatives (LacdiNAc) (20) were prepared with sequence-defined sugar densities (16, 17). These JGDs self-assembled into monodisperse nanoscale glycodendrimersomes (GDSs) after injecting their ethanol or tetrahydrofuran solution into buffer (10, 14–20). The resulting GDSs agglutinate with plant (14–16) or bacterial lectins (14, 15), as well as human galectins (14, 15, 17–20), and thus provide a toolbox to unveil the relationship between different glycan structures, densities, and affinities on the cell-mimic surface for lectins and galectins. Bicomponent raft-like domains with lamellar or hexagonal nanoscale morphologies on

Significance

Synthetic macromolecules that mimic glycolipids, named Janus glycodendrimers (JGDs), have been shown to self-assemble into nanoscale vesicles displaying glycans on their outer surface, similar to the glycocalyx coating of eukaryotic cells, bacteria, and viruses. Specifically, both linear and branched oligosaccharides synthesized by automated glycan assembly, with hydrophobic linkers, have been used to create JGDs via an isothiocyanate-amine coupling reaction. Surprisingly, in spite of the hydrophobic linker, these JGDs self-organize into nanovesicles exhibiting lamellar surface morphologies, which mimic the recognition structures of cell-surface glycans and viral glycoproteins. Therefore, they are likely to be useful in helping elucidate mechanisms of significance for translational medicine such as the camouflage functionality employed by viruses to evade recognition.

Author contributions: P.H.S. and V.P. designed research; Q.X., M.D., S.E.S., A.M.R.P., P.B., A.P.-V., C.R.-E., N.Y.K., K.R., and D.S. performed research; M.M. contributed new reagents/analytic tools; Q.X., M.D., S.E.S., C.R.-E., N.Y.K., K.R., D.S., M.L.K., P.H.S., and V.P. analyzed data; and Q.X., M.D., S.E.S., C.R.-E., M.L.K., P.H.S., and V.P. wrote the paper.

Reviewers: J.R.K., University of Utah; and L.P., Aix-Marseille Université and CNRS.

The authors declare no competing interest.

This open access article is distributed under [Creative Commons Attribution-NonCommercial-NoDerivatives License 4.0 \(CC BY-NC-ND\)](https://creativecommons.org/licenses/by-nc-nd/4.0/).

¹To whom correspondence may be addressed. Email: mklein@temple.edu, peter.seeberger@mpikg.mpg.de, or percec@sas.upenn.edu.

This article contains supporting information online at <https://www.pnas.org/lookup/suppl/doi:10.1073/pnas.2003938117/-DCSupplemental>.

First published May 18, 2020.

the surface of GDSs were shown to bind more effectively at low sugar concentrations (18).

To date, most JGDs (14–20) have been synthesized via copper-catalyzed azide–alkyne cycloadditions (CuAAC) usually known as the conventional click reaction (21, 22) involving simple mono- or disaccharides bearing azido or alkyne moieties (14–20). A detailed investigation of the design principles of JGDs demonstrated through seven libraries containing 51 JGDs that hydrophilic linkers containing three to four oligo(oxyethylene)s must be connected directly to the sugar while the triazole group formed by click should be attached directly to the hydrophilic part of the dendron (14). These principles were used to design and predict the primary structure of self-assembling JGDs (15–20). Longer oligosaccharides have not been conjugated to JDs due to the difficulties associated with their synthesis and further conjugation by conventional CuAAC click reactions.

Automated glycan assembly (AGA) (23–25) has expedited access to well-defined complex glycans up to 100-mers (24) that can serve as molecular tools for glycoscience (26). Synthetic oligosaccharides obtained by AGA are stereochemically pure and are equipped with an *N*-pentyl amino hydrophobic linker that facilitates the conjugation to surfaces or biomolecules (23–25). This hydrophobic *N*-pentyl amino linker attached to oligosaccharides prepared by AGA in milligram quantities does not fulfill the most fundamental structural requirement for the construction of JGDs by the classic click chemistry already elaborated (14). Fortunately, control experiments have demonstrated that a thiourea group incorporated between the hydrophobic link of the sugar and the hydrophilic part of the dendrimer via an isothiocyanate (ITC) “click”-like reaction provides JGDs that self-assemble into GDSs. Herein, we report that synthetic glycans obtained by AGA have been conjugated

to JGDs via an ITC–amine “click”-like methodology to enable their self-organization into GDSs that mimic biological membranes.

Results and Discussion

A representative example for the synthesis of a disaccharide Lac containing a triethylene glycol linker with an azido group is presented in Fig. 1A (19). Glycosylation of 2-(2-[2-chloroethoxy]ethoxy)ethan-1-ol (**2**) with lactose octa-acetate (**1**) catalyzed by the Lewis acid boron trifluoride etherate ($\text{BF}_3 \cdot \text{OEt}_2$) generates compound **3**, equipped with triethylene glycol chloride linker. The azido substituted compound **4** was synthesized upon treatment with sodium azide at 80 °C in dimethylformamide (DMF). The acetyl groups were removed via Zemplén deacetylation with sodium methoxide in methanol to give compound **5**. Hydrogenation in the presence of Pd/C provided Lac bearing a triethylene glycol chain with an amino group (**6**). The synthesis of Lac functionalized with the hydrophobic amino-pentyl linker (**10**) (**27**) started when lactose octaacetate (**1**) was first reacted with hydrazine acetate, followed by treatment with trichloroacetonitrile and 1,8-diazabicyclo[5.4.0]undec-7-ene (DBU) to give **7**. Intermediate **7** was functionalized with benzyl (5-hydroxypentyl)carbamate (**8**) to generate **9** (Fig. 1B). After Zemplén deacetylation and hydrogenolysis of the carboxybenzyl (Cbz) group of **9**, Lac containing the amino-pentyl linker (**10**) was obtained.

AGA of hexaMan (Fig. 1C) is representative for the synthesis of all oligoMan (23–25) (*SI Appendix, Figs. S1–S32*). AGA was performed with thiomannoside (**11**) on a polymeric resin functionalized with a photo-cleavable linker (**12**). Six cycles of glycosylation and deprotection were repeated to obtain the desired hexa-saccharide. Upon completion of the assembly, the compound was cleaved from the solid support and subjected to Zemplén methanolysis and hydrogenolysis to give compound hexaMan (**13**).

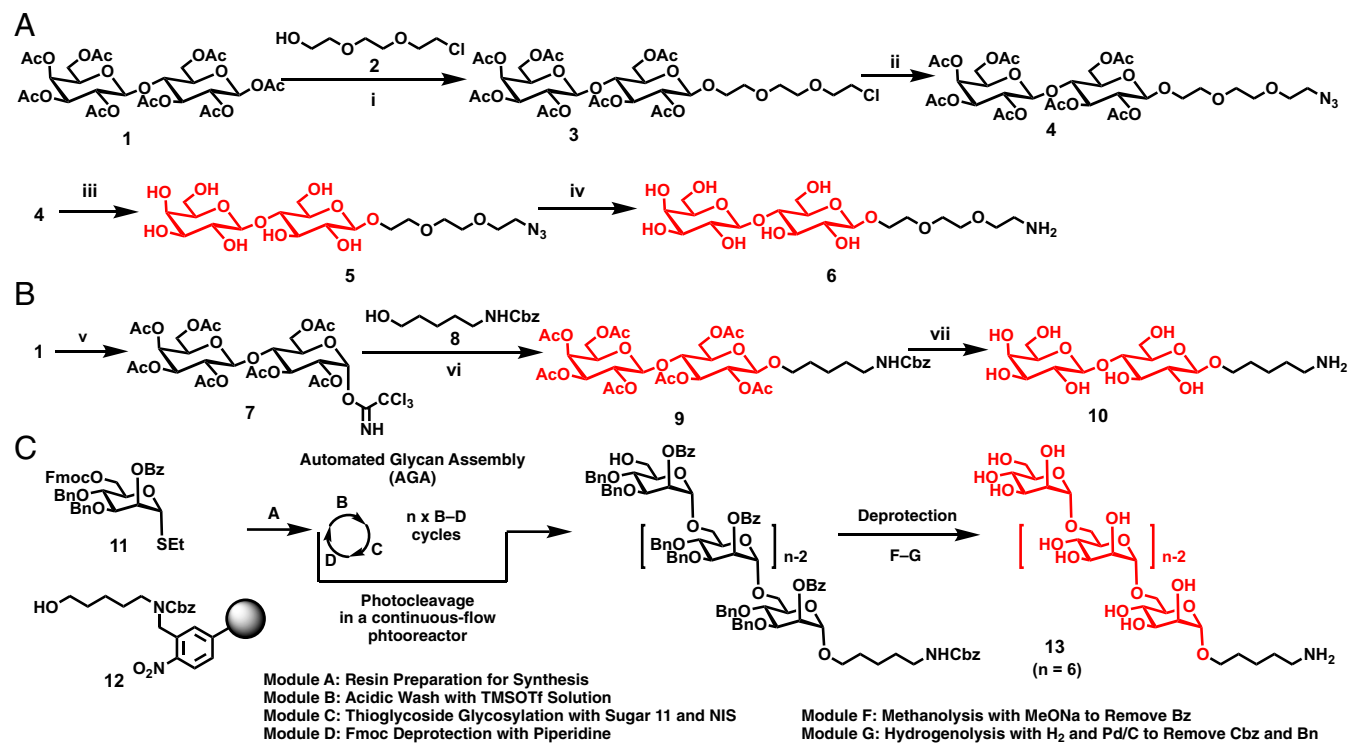


Fig. 1. Synthetic route for preparation of sugars containing triethylene glycol azido and amino linkers (A). Synthetic route for sugar containing the hydrophobic *N*-pentyl amino linkers (B). Automated glycan assembly of oligoMan containing *N*-pentyl amino linkers (C). Reagents and conditions: (i) $\text{BF}_3 \cdot \text{Et}_2\text{O}$, CH_2Cl_2 , 0 °C to 23 °C, 15 h, 80%; (ii) NaN_3 , DMF, 80 °C, 15 h, 74%; (iii) MeONa, methanol, pH = 10, 23 °C, 7 h, 95%; (iv), H₂, Pd/C, methanol, 23 °C, 15 h, 95%; (v) $\text{H}_2\text{NNH}_2 \cdot \text{HOAc}$, DMF, then CCl_3CN , DBU, CH_2Cl_2 , 79%; (vi) TMSOTf, CH_2Cl_2 , 39%; (vii) MeONa, methanol, then H₂, Pd/C, 82%.

The AGA of oligoMan is usually performed on a 0.0125-mmol scale and therefore requires a highly efficient methodology to conjugate this small quantity of oligosaccharides to the JGDs. In order to selectively conjugate the primary amino group to the JGDs in the presence of multiple hydroxyl groups and to potentially diminish the hydrophobic character of oligoMan linker, the incorporation of an alkyl ITC on the hydrophilic part of JD was designed. ITC reacts with amines fast and irreversibly, while the reaction between ITC and alcohols and even water, which can be used also as a solvent, is negligible and reversible (28), being below the level that can be detected by analytical methods. Due to this selectivity, ITC functionalized compounds are widely used for orthogonal bioconjugation (28, 29) and Sharpless and coworkers (21) considered this reaction as part of the large protocol of click methods. In addition,

as it will be discussed later, the Lac-containing hydrophilic and hydrophobic linkers were used to produce the model compounds **5**, **6**, and **10**. They all formed JGDs that self-assemble in GDSs with similar stability in buffer and efficiency to agglutination. Therefore, the ITC-amine “click”-like reaction was preferred since it did not require any change to the current AGA technology.

The synthesis of ITC functionalized JD is presented in Fig. 2. The 2-(2-[2-chloroethoxy]ethoxy)ethan-1-ol (**2**) was reacted with sodium azide to obtain 2-[2-(2-azidoethoxy)ethoxy]ethanol (**14**), followed by chlorination with thionyl chloride to generate 1-azido-2-(2-[2-chloroethoxy]ethoxy)ethane (**15**) (30). Alkylation of methyl 4-(benzyloxy)-3,5-dihydroxybenzoate (**16**), followed by deprotection and alkylation, provided the azido-functionalized hydrophilic minidendron (**21**). The hydrophilic minidendron (**22**)

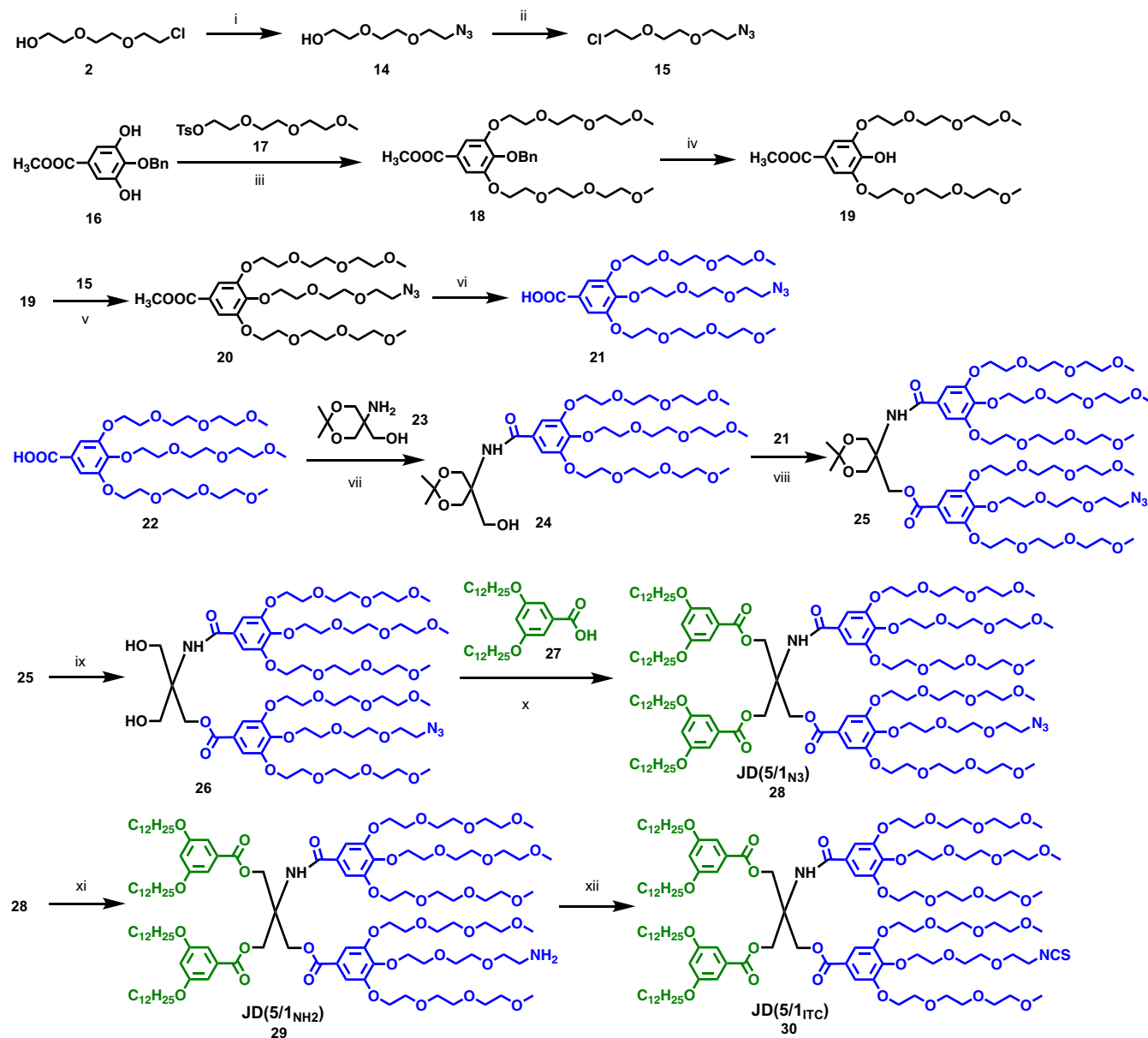


Fig. 2. Synthesis of ITC functionalized JD. Reagent and conditions: (i) NaN_3 , DMF, 15 h, 85 °C; (ii) SOCl_2 , benzyltriethylammonium chloride (BTEAC), 65 °C, 2 h, 93% for 2 steps; (iii) K_2CO_3 , DMF, 80 °C, 48 h, 94%; (iv) H_2 , Pd/C, methanol, 55 °C, 15 h, 100%; (v) K_2CO_3 , 18-C-6, DMF, 80 °C, 15 h, 90%; (vi) KOH, ethanol, 90 °C, 2 h, then 2 M HCl, 100%; (vii) CDMT, NMM, THF, 12 h, 93%; (viii) DCC, DPTS, CH_2Cl_2 , 23 °C, 24 h, 80%; (ix) 2 M HCl, methanol, 23 °C, 2 h, 98%, (x) DCC, DPTS, CH_2Cl_2 , 23 °C, 24 h, 93%; (xi) H_2 , Pd/C, methanol, 12 h, 81%; (xii) CS_2 , NEt_3 , THF, 0 °C, then TsCl, 23 °C, 95%.

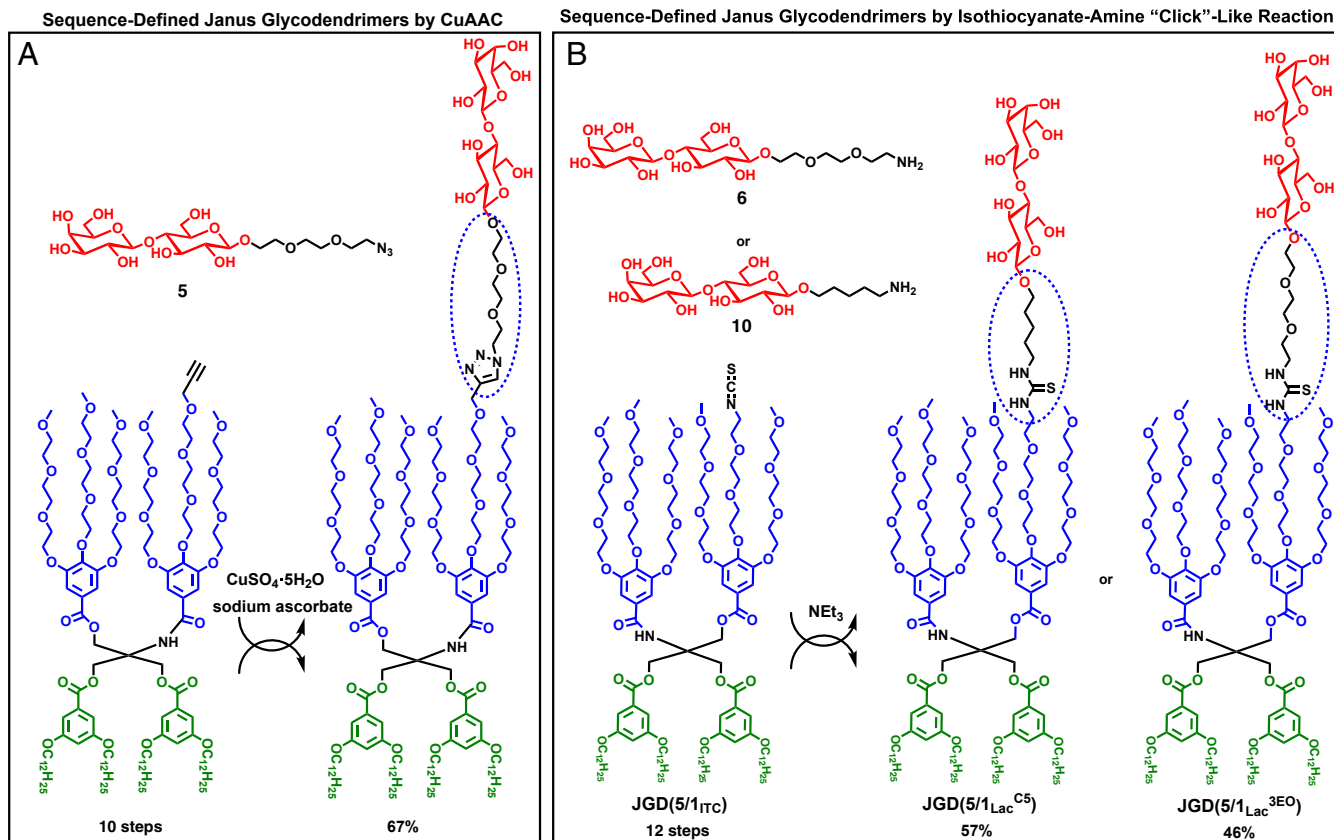


Fig. 3. Sequence-defined JGDs obtained by conventional click reaction via CuAAC (20) (A) and by ITC-amine "click"-like reaction (B), reported here.

was connected to the acetone-protected Tris(hydroxymethyl)-aminomethane (Tris) core (**23**) with 2-chloro-4,6-dimethoxy-1,3,5-triazine (CDMT) and *N*-methylmorpholine (NMM), followed

by conjugation with the azido functionalized hydrophilic mini-dendron (**21**) via *N,N'*-dicyclohexylcarbodiimide (DCC) and 4-(dimethylamino)pyridinium 4-toluenesulfonate (DPTS) (31).

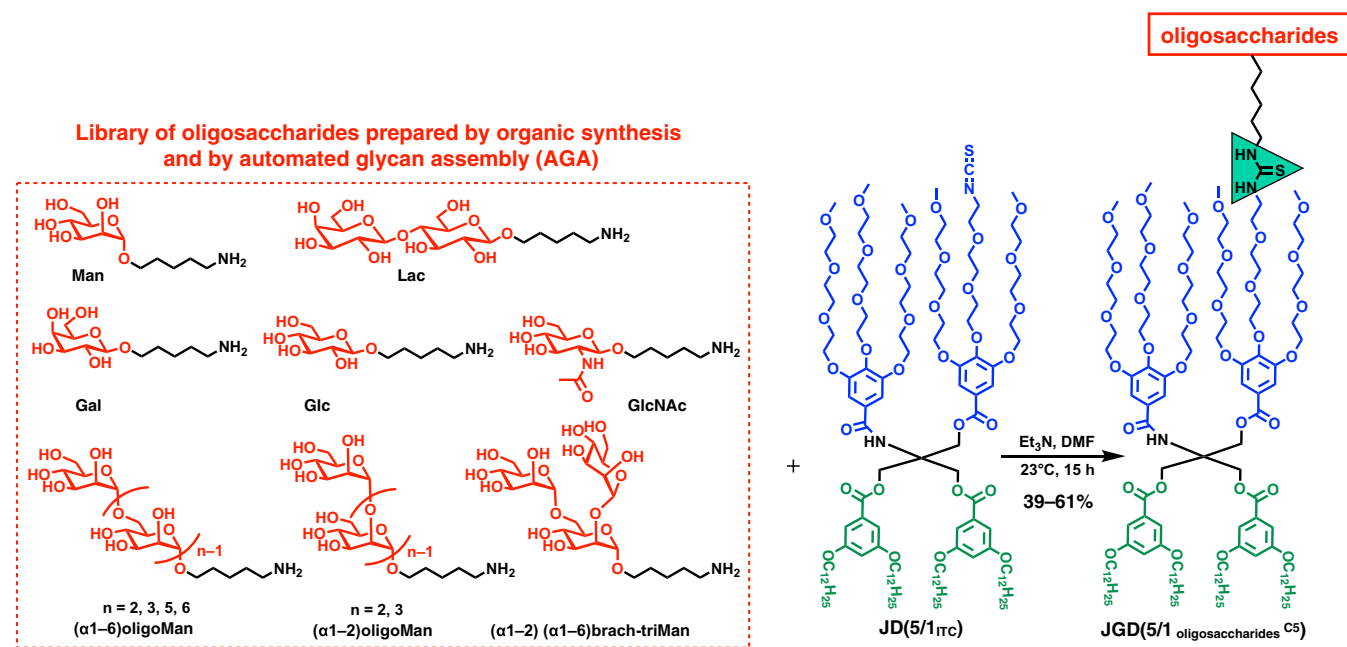


Fig. 4. Oligosaccharides with pentyl-amino linker used for the preparation of JGDs via ITC-amine "click" reaction. Man and Lac were prepared by solution phase synthesis. Man, Gal, Glc, GlcNAc, and oligoMan were prepared by AGA.

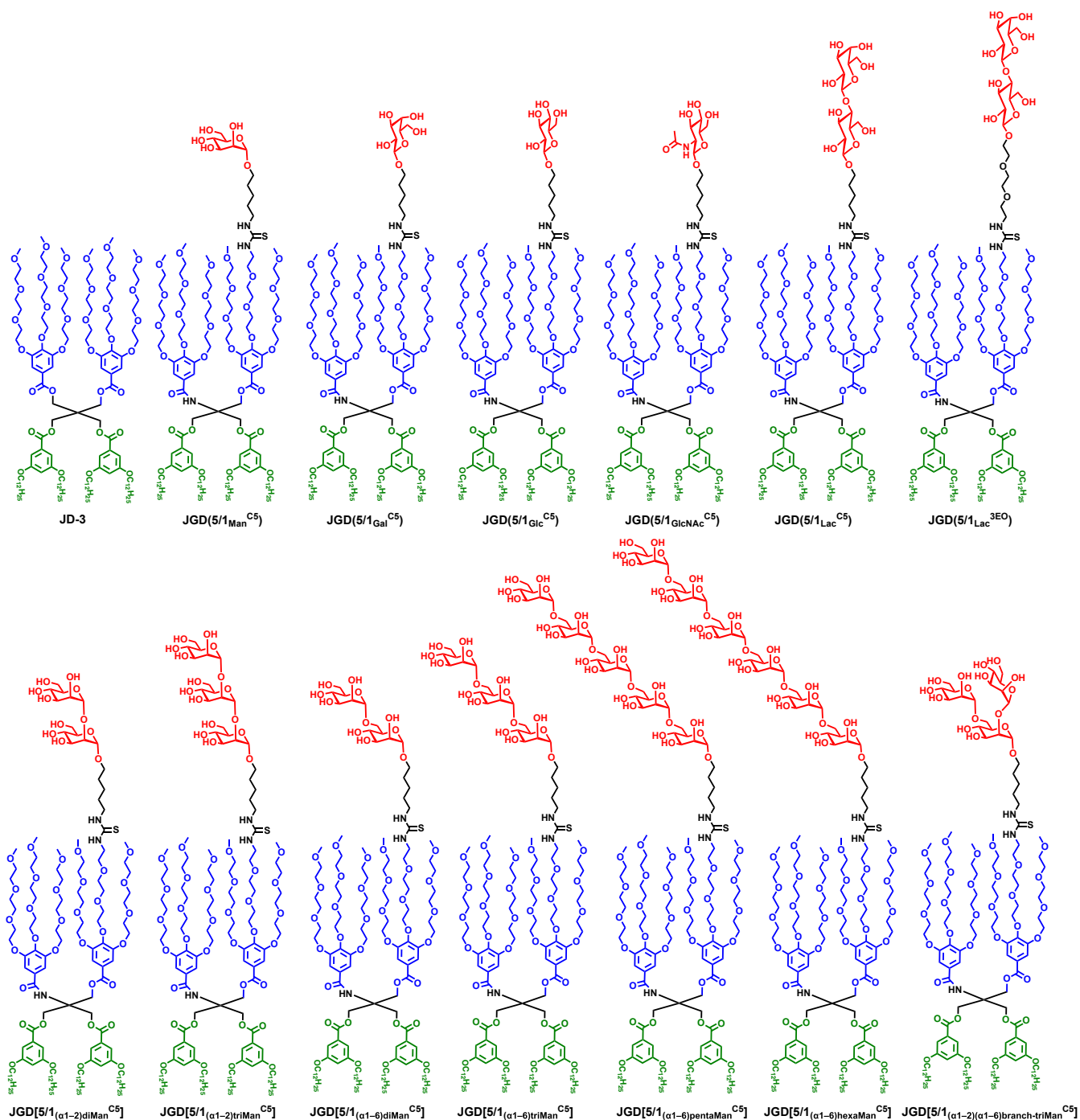


Fig. 5. Library of sequence-defined amphiphilic JGDs containing monosaccharide (Man, Gal, Glc, and GlcNAc), disaccharide (Lac), and oligoMan. An amphiphilic JD, JD-3 (8), which was coassembled with JGDs, is presented in the top row, left side.

Upon deprotection of the acetonide and conjugation to the hydrophobic minidendron (27) with DCC and DPTS, the azido containing amphiphilic JD [**JD(5/1_{N3})**, 28] was obtained. The nomenclature of **JD(5/1_{N3})** was adapted from that of sequence-defined JGDs elaborated by our laboratory (18). For example, 5/1 corresponds to five methyl triethylene glycol chains and one azido (N_3) functionalized triethylene glycol chain on the hydrophilic dendrons of sequence-defined JD. The azido group of **JD(5/1_{N3})** was reduced to amine by hydrogenation to obtain **JD(5/1_{NH2})** (29). Finally, an efficient method using carbon disulfide (32), triethyl amine, and tosyl chloride was

employed to transform the amino group to ITC under mild conditions and produce the ITC functionalized sequence-defined JD **JD(5/1_{ITC})** (30). Tosyl chloride was used to mediate decomposition of the corresponding dithiocarbamate salt which was generated in situ by treatment of the amine **JD(5/1_{NH2})** with carbon disulfide and triethylamine (32). The formation of the azido and ITC-containing JDs was confirmed by NMR and matrix-assisted laser desorption ionization time-of-flight (MALDI-TOF) mass analysis (*SI Appendix, Fig. S33*).

Disaccharides 6 and 10 were selected as models to test the ITC–amine “click” conjugation with ITC functionalized JD

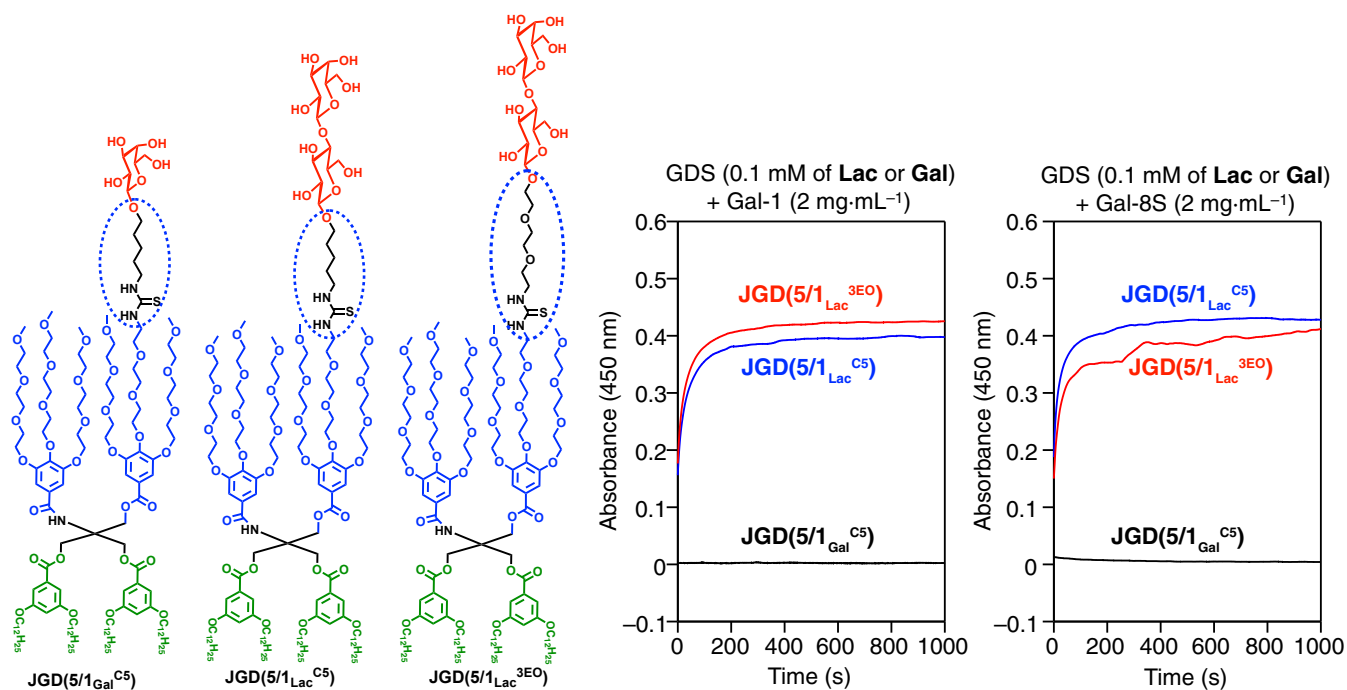


Fig. 6. GDSs self-assembled from JGDs containing Gal and Lac prepared by ITC-amine “click” reaction with pentyl (C5) or triethylene glycol (3EO) linkers and their agglutination with human galectin-1 (Gal-1) and galectin-8S (Gal-8S).

JD(5/1_{ITC}) (30), in the presence of triethyl amine and DMF. The conventional click reaction via CuAAC (18) was previously utilized to synthesize sequence-defined JGDs (Fig. 3A) (14–20). Copper sulfate was reduced in situ with sodium ascorbate to catalyze the azide-alkyne cycloaddition and form a 1,2,3-triazole ring that connected the JD with the sugar. Similarly, the ITC-amine “click”-like reaction occurred between the ITC group of the **JD(5/1_{ITC}) (30)** and the amine of the Lac analogs **6**, containing a triethylene glycol linker (3EO), and **10**, containing the hydrophobic *N*-pentyl linker (C5) (Fig. 3B) where thiourea connected the hydrophilic JD and the hydrophobic part of the sugar. Two JGDs containing sequence-defined Lac 3EO hydrophilic chain **JD(5/1_{Lac}^{3EO})** and sequence-defined Lac 3EO hydrophilic chain **JD(5/1_{Lac}^{C5})** were successfully synthesized in 57% and 46% isolated yields from Lac analogs **6** or **10**, respectively. This reaction is competitive with the conventional click chemistry (compare isolated yields in Fig. 3A and B) except that the as obtained from AGA hydrophobic *N*-pentyl linked amine is used directly in the ITC-amine “click”-like reaction and therefore it does not require any additional synthetic steps.

The ITC-amine “click”-like methodology was employed to build a library of JGDs containing oligosaccharides (Fig. 4). Amino-pentyl functionalized Man and Lac were prepared by conventional solution phase synthesis (Fig. 1B). Man, Gal, Glc, *N*-acetylglucosamine (GlcNAc), and oligoMan, including (α1-6)-type diMan, triMan, pentaMan, hexaMan; (α1-2)-type diMan and triMan; and (α1-2) (α1-6) branched-triMan were prepared by AGA (*SI Appendix*, Figs. S1–S32). The sugars were mixed with **JGD(5/1_{ITC})** in DMF in the presence of triethyl amine. DMF was selected as the solvent due to good solubility for both ITC-containing JD **JGD(5/1_{ITC})** and amino-containing sugars. The target JGDs were purified on silica gel chromatography with CH₂Cl₂/methanol (for JGDs containing mono- to trisaccharides) or CH₂Cl₂/methanol/water (for JGDs containing more than trisaccharides) as eluents to give the desired products in 39 to 61% isolated yields without any optimization (Fig. 4).

This reaction can be efficiently performed even with only few milligrams of sugar as obtained by AGA and confirmed by

MALDI-TOF analysis (*SI Appendix*, Figs. S34 and S35). Due to the solubility of the less-polar JD part, the amphiphilic JGDs can be dissolved in less-polar NMR solvents such as CDCl₃, where the JGDs did not self-assemble. The chemical structures of sequence-defined amphiphilic JGDs containing monosaccharide (Man, Gal, Glc, and GlcNAc), disaccharide as Lac, and linear or branched oligoMan are summarized and compared in Fig. 5.

GDSs were assembled by injecting tetrahydrofuran solutions of JGDs in water or buffer, as reported previously (14–20). Cryogenic transmission electron microscopy analysis (*SI Appendix*, Fig. S36), of these GDSs self-organized from JGDs containing Lac and oligoMan via ITC-amine “click” reaction demonstrated the formation of unilamellar vesicles with a diameter of about 100 nm. The self-assembled GDSs are similar to those previously reported GDSs when they were prepared via the CuAAC click method (14–20). This is a remarkable result considering that JDSs containing hydrophobic linkers attached to the sugar do not form GDSs (14). This demonstrates the extraordinary contribution of the thiourea interconnecting group between the hydrophobic and hydrophilic fragments of JDSs to their self-assembly. Therefore, these experiments demonstrated the efficiency of the ITC-amine “click”-like reaction for the synthesis of amphiphilic JGDs containing complex oligosaccharides.

In order to investigate the activity of sugars on the surface of JGDs, we self-assembled GDSs from **JGD(5/1_{Gal}^{C5})**, **JGD(5/1_{Lac}^{C5})**, and **JGD(5/1_{Lac}^{3EO})** in 1× phosphate-buffered saline (Fig. 6). The agglutination assays were performed with these GDSs with two adhesion/growth-regulatory human galectins: galectin-1 (Gal-1) (18) and galectin-8S (Gal-8S) (17, 18). Human galectins bind to the disaccharide Lac much stronger than monosaccharide Gal. Gal-containing GDSs did not show increase of turbidity, most probably due to the weak interaction between the two components. In contrast, the two GDSs with Lac showed similar agglutination behavior with Gal-1 and Gal-8S. These data indicated the similar activity of the sugars on the surface of GDSs regardless of the presence of the hydrophilic triethylene glycol or hydrophobic

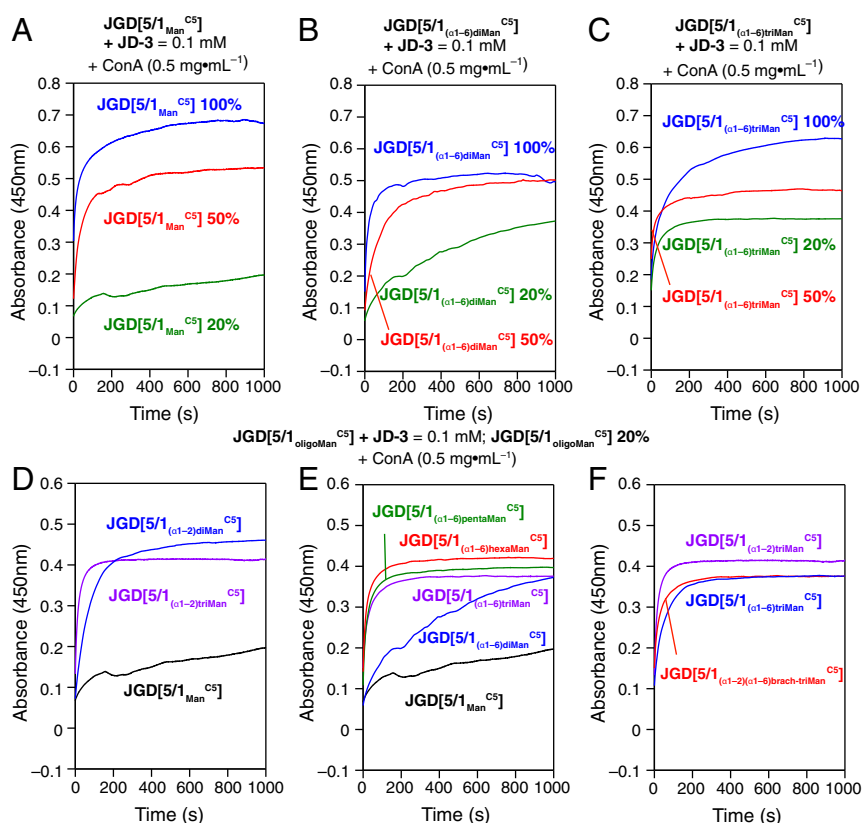


Fig. 7. Agglutination assays of GDSs from amphiphilic JGDs containing oligoMan with ConA. (A–C) Agglutination assays of GDS from JGDs containing Man (A), diMan (B), and triMan (C). The GDSs were prepared by self-assembly of the JGDs (100%) or coassembled with JD-3 (20 and 50 mol % of JGDs). (D and E) Agglutination assays of GDS from JGDs containing (α 1–2) oligoMan (D), (α 1–6) oligoMan (E), and comparison of three JGDs containing isomeric linear or branched trimannose (F). The GDSs were prepared by coassembled with JD-3 (20 mol % of JGDs).

N-pentyl linker connected to the hydrophilic fragment via thiourea (see ovoidal dashed structures in Figs. 3 A and B and 6). Thus, complex carbohydrates containing the hydrophobic pentyl linker attached to hydrophobic fragments via thiourea can be used

to design self-assembling JGDs (14). This demonstrates that the thiourea group incorporated during the ITC–amine “click”-like reaction enhances the hydrophilic character of the *N*-pentyl linker and facilitates the self-assembly process of the JGDs.

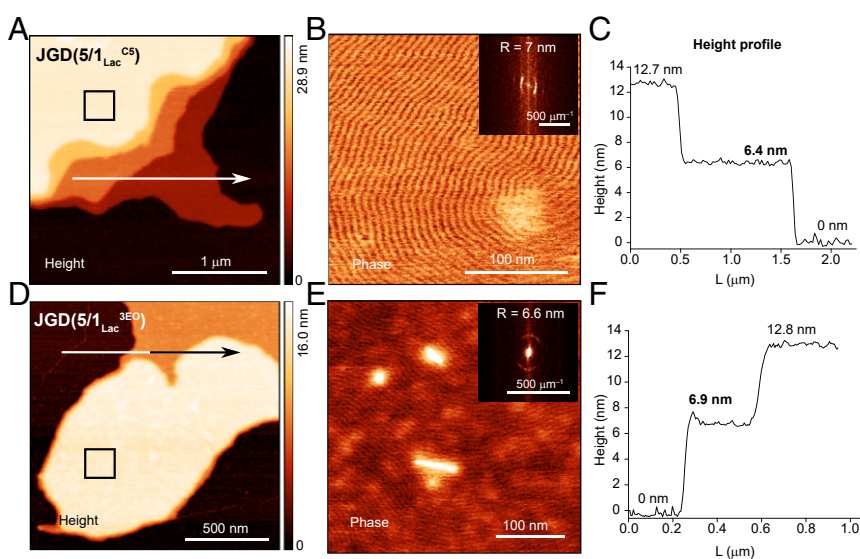


Fig. 8. Surface topography of GDS self-organized from Lac-containing sequence-defined JGDs including JGD(5/1_{Lac}^{C5}) (A–C) with a hydrophobic C5 linker and JGD(5/1_{Lac}^{3EO}) (D–F) with a hydrophilic 3EO linker deposited on mica. AFM height images (A and D), phase images (B and E) with inserted FFT, and the corresponding height profiles (C and F) of GDSs on mica measured at ambient humidity (40%). Arrows in A and D indicate the directions for analysis of the height profiles in C and F.

GDSs self-organized from JGDs containing oligoMan were assembled by injection into 4-(2-hydroxyethyl)-1-piperazineethanesulfonic acid (Hepes) buffer containing CaCl₂ and MnCl₂. Agglutination experiments of the GDSs from Man (Fig. 7A), (α1–6) diMan (Fig. 7B), and (α1–6) triMan (Fig. 7C) with concanavalin A (ConA) (14, 16) were performed. Tetrameric leguminous lectin ConA binds to Man and oligosaccharides containing terminal Man units, in the presence of Ca²⁺ and Mn²⁺ (7, 9, 10, 12). These GDSs aggregated with ConA, indicating the existence of (α1–6)-type oligoMan on the surface of GDSs. However, the binding curves (blue curves, Fig. 7A–C) did not correlate the different numbers of the (α1–6) oligoMan units. Therefore, JGDs were coassembled in the presence of a nonsugar JD (JD-3, Fig. 5, top left row). The ratio of JGDs was diluted from 100 to 50% (red curves, Fig. 7A–C) and to 20% (green curves, Fig. 7A–C). For Man (Fig. 7A), the green curve (20%) is much lower than the blue curve (100%). In contrast, for triMan (Fig. 7C), the green curve (20%) maintained at a relative high level. The coassembled GDSs with 20% JGDs showed an increased trend with an increasing number of (α1–6) oligoMan units (green curves in Fig. 7A–C, and in Fig. 7E). Thus, the coassembled GDSs containing 20% of JGDs can be employed to investigate the relative activity of JGDs in the biological membrane mimic with the function of oligoMan units. Based on these results, we prepared the coassembled GDSs including 20% JGDs and 80% of JD-3 (see structure of JD-3 in Fig. 5, top left row) for the entire oligoMan-containing JGDs library (Fig. 7D–F). For (α1–2) oligoMan, the slopes of binding curves increased with each lengthening of the sugar from Man to (α1–2) diMan and then to (α1–2) triMan (Fig. 7D). Fig. 7E demonstrated the hexaMan containing JGD is the most active among the (α1–6) oligoMan. Three triMan-containing JGDs with linear (α1–2) triMan, linear (α1–6) triMan, or (α1–2) (α1–6) branch-triMan, showed the highest slopes as well as plateau (Fig. 7F). It should be noted that all oligoMan-presenting GDSs demonstrated higher activity toward ConA whether linear or branched than the monosaccharide Man-presenting GDSs. Therefore, the synthesis of JGDs from unprotected sugars performed under the ITC–amine “click”-like reaction conditions provides an efficient methodology to combine AGA-generated small quantities of complex-architecture oligosaccharides with GDSs to yield synthetic cell-like objects decorated with sugar moieties.

Analysis using a combination of atomic force microscopy (AFM) and fast Fourier transform (FFT) with a diffraction-like method of the semidried GDSs on mica, demonstrated stage-like membrane bilayers in the GDS (18). Lac-containing JGDs showed bilayer thicknesses of about 6.5 nm (Fig. 8). Raft-like (33, 34) lamellar periodic nanopatterns (Fig. 8) demonstrated the organization of sugars on the surface of GDSs, similar to Lac-based JGDs (18). Similar lamellar morphologies on GDSs from linear oligoMan, including hexaMan-containing JGDs, were also observed (SI Appendix, Fig. S37).

Conclusions

The synthesis of JGDs bearing complex oligosaccharides with a hydrophobic amine linker via an ITC–amine “click”-like reaction provided results comparable to the use of the azide–alkyne click reaction, previously employed to prepare JGDs with oligosaccharides containing an hydrophilic oligo(ethylene

oxide) linker (14). Model reactions with Lac-containing hydrophobic or hydrophilic linkers demonstrated that the hydrophobic amino-linker incorporated at the reducing end of complex carbohydrates synthesized by AGA is compatible with the method based on hydrophilic tri- or tetraethylene glycol amino or azido groups. The thiourea hydrophilic fragment introduced in the hydrophobic part by the ITC–amine “click”-like reaction balances the hydrophobicity of the linker. This is a surprising result considering that the hydrophobic linkers attached to sugars do not form JGDs that self-assemble into GDSs (14). Therefore, additional experiments are needed to generalize this concept, which may endow a new architectural approach to JGD and GDSs. Oligosaccharides prepared by AGA (23–25), including a linear oligoMan with six mannose units and a branched trimannose, were conjugated to JDs via ITC–amine “click”-like without any additional synthetic modification of the carbohydrate. The resulting JGDs self-assembled into unilamellar GDSs. OligoMan-containing GDSs bind the mannose-binding lectin ConA, with the hexaMan binding the most tightly. Some GDSs adopt raft-like nanomorphologies on their cell-membrane mimic surface to support the enhanced activity previously observed for other sequence-defined GDSs (17, 18, 19) and hence shed light on the relationship between glycan structure and activity. The combination of AGA and the self-organization of sequence-defined JGDs has created models to start illuminating why biological cell membranes carry long and branched glycans, which are bound more tightly by sugar-binding proteins. These results provide a platform to develop cell-membrane mimics and the tools required to conjugate amino containing biomacromolecules to JDs, including not only more complex carbohydrates synthesized by AGA but also peptides and oligonucleotides.

The combined synthetic ITC–amine conjugation (28, 29) and AGA (23–25) with supramolecular multivalency (35, 36) methodology reported here by the assembly of GDSs based on oligoMan (37–39) provides a pathway to investigate the mechanism of action of even more complex naturally occurring glycans and develop applications in translational medicine. Last, but not least, since viruses are coated with linear and branched oligoMan, the blending of AGA with JGD and GDS methodologies reported here is likely to help elucidate the function of glycan camouflaging employed by viruses (40, 41).

Methods

Glycan Synthesis. AGA was performed on a home-built synthesizer developed at the Max Planck Institute of Colloids and Interfaces, Goltm, Germany (25). All details concerning preautomation steps, building blocks, AGA modules, and postsynthesizer manipulations can be found in SI Appendix.

Data Availability. All data associated with this work are available either in the main text or in SI Appendix.

ACKNOWLEDGMENTS. This work was supported by NSF Grants DMR-1807127 and DMR-1720530, the P. Roy Vagelos Chair at the University of Pennsylvania (all to V.P.), the Alexander von Humboldt Foundation (to N.Y.K. and V.P.), the Max Planck Society and the Minerva Fast Track Program, the Max-Planck-Gesellschaft–Fraunhofer-Gesellschaft Cooperation Project Glyco3Display and the Deutsche Forschungsgemeinschaft (SFB1340 “Matrix-in Vision”) (to M.D. and P.H.S.), Sheikh Saqr Research Foundation (to M.L.K.), and H2020-NMBP-TR-IND-2018, EVPRO (Development of Extracellular Vesicles loaded hydrogel coatings with immunomodulatory activity for Promoted Regenerative Osseointegration of revision endoprostheses) Grant 814495-2 (to C.R.-E. and N.Y.K.).

1. A. D. Bangham, M. M. Standish, J. C. Watkins, Diffusion of univalent ions across the lamellae of swollen phospholipids. *J. Mol. Biol.* **13**, 238–252 (1965).
2. H. Ringsdorf, B. Schlarb, J. Venzmer, Molecular architecture and function of polymeric oriented systems: Models for the study of organization, surface recognition, and dynamics of biomembranes. *Angew. Chem. Int. Ed. Engl.* **27**, 113–158 (1988).
3. J. L. Thomas, D. A. Tirrell, Polyelectrolyte-sensitized phospholipid vesicles. *Acc. Chem. Res.* **25**, 336–342 (1992).
4. T. Kunitake, Synthetic bilayer membranes: Molecular design, self-organization, and application. *Angew. Chem. Int. Ed. Engl.* **31**, 709–726 (1992).
5. X. Guo, F. C. Szoka Jr., Chemical approaches to triggerable lipid vesicles for drug and gene delivery. *Acc. Chem. Res.* **36**, 335–341 (2003).
6. B. M. Discher et al., Polymersomes: Tough vesicles made from diblock copolymers. *Science* **284**, 1143–1146 (1999).
7. D. E. Discher, A. Eisenberg, Polymer vesicles. *Science* **297**, 967–973 (2002).

8. V. Percec *et al.*, Self-assembly of Janus dendrimers into uniform dendrimersomes and other complex architectures. *Science* **328**, 1009–1014 (2010).
9. M. Peterca, V. Percec, P. Leowanawat, A. Bertin, Predicting the size and properties of dendrimersomes from the lamellar structure of their amphiphilic Janus dendrimers. *J. Am. Chem. Soc.* **133**, 20507–20520 (2011).
10. S. E. Sherman, Q. Xiao, V. Percec, Mimicking complex biological membranes and their programmable glycan ligands with dendrimersomes and glycodendrimersomes. *Chem. Rev.* **117**, 6538–6631 (2017).
11. Q. Xiao *et al.*, Bioactive cell-like hybrids coassembled from (glyco)dendrimersomes with bacterial membranes. *Proc. Natl. Acad. Sci. U.S.A.* **113**, E1134–E1141 (2016).
12. S. S. Yadavalli *et al.*, Bioactive cell-like hybrids from dendrimersomes with a human cell membrane and its components. *Proc. Natl. Acad. Sci. U.S.A.* **116**, 744–752 (2019).
13. P. Torre *et al.*, Encapsulation of hydrophobic components in dendrimersomes and decoration of their surface with proteins and nucleic acids. *Proc. Natl. Acad. Sci. U.S.A.* **116**, 15378–15385 (2019).
14. V. Percec *et al.*, Modular synthesis of amphiphilic Janus glycodendrimers and their self-assembly into glycodendrimersomes and other complex architectures with bioactivity to biomedically relevant lectins. *J. Am. Chem. Soc.* **135**, 9055–9077 (2013).
15. S. Zhang *et al.*, Mimicking biological membranes with programmable glycan ligands self-assembled from amphiphilic Janus glycodendrimers. *Angew. Chem. Int. Ed. Engl.* **53**, 10899–10903 (2014).
16. Q. Xiao *et al.*, Onion-like glycodendrimersomes from sequence-defined Janus glycodendrimers and influence of architecture on reactivity to a lectin. *Proc. Natl. Acad. Sci. U.S.A.* **113**, 1162–1167 (2016).
17. S. Zhang *et al.*, Glycodendrimersomes from sequence-defined Janus glycodendrimers reveal high activity and sensor capacity for the agglutination by natural variants of human lectins. *J. Am. Chem. Soc.* **137**, 13334–13344 (2015).
18. C. Rodriguez-Emmenegger *et al.*, Encoding biological recognition in a bicomponent cell-membrane mimic. *Proc. Natl. Acad. Sci. U.S.A.* **116**, 5376–5382 (2019).
19. Q. Xiao *et al.*, Exploring functional pairing between surface glycoconjugates and human galectins using programmable glycodendrimersomes. *Proc. Natl. Acad. Sci. U.S.A.* **115**, E2509–E2518 (2018).
20. A.-K. Ludwig *et al.*, Design-functionality relationships for adhesion/growth-regulatory galectins. *Proc. Natl. Acad. Sci. U.S.A.* **116**, 2837–2842 (2019).
21. H. C. Kolb, M. G. Finn, K. B. Sharpless, Click chemistry: Diverse chemical function from a few good reactions. *Angew. Chem. Int. Ed. Engl.* **40**, 2004–2021 (2001).
22. V. V. Rostovtsev, L. G. Green, V. V. Fokin, K. B. Sharpless, A stepwise Huisgen cycloaddition process: Copper(I)-catalyzed regioselective "ligation" of azides and terminal alkynes. *Angew. Chem. Int. Ed. Engl.* **41**, 2596–2599 (2002).
23. M. Guberman, P. H. Seeberger, Automated glycan assembly: A perspective. *J. Am. Chem. Soc.* **141**, 5581–5592 (2019).
24. A. A. Joseph, A. Pardo-Vargas, P. H. Seeberger, Total synthesis of polysaccharides by automated glycan assembly. *J. Am. Chem. Soc.*, 10.1021/jacs.0c00751 (2020) In press.
25. M. Delbianco *et al.*, Well-defined oligo- and polysaccharides as ideal probes for structural studies. *J. Am. Chem. Soc.* **140**, 5421–5426 (2018).
26. M. W. Weishaupt *et al.*, Automated glycan assembly of a *S. pneumoniae* serotype 3 CPS antigen. *Beilstein J. Org. Chem.* **12**, 1440–1446 (2016).
27. C. Wendeln, A. Heile, H. F. Arlinghaus, B. J. Ravoo, Carbohydrate microarrays by microcontact printing. *Langmuir* **26**, 4933–4940 (2010).
28. O. Koniev, A. Wagner, Developments and recent advancements in the field of endogenous amino acid selective bond forming reactions for bioconjugation. *Chem. Soc. Rev.* **44**, 5495–5551 (2015).
29. J. L. Riggs, R. J. Seiwald, J. H. Burckhalter, C. M. Downs, T. G. Metcalf, Isothiocyanate compounds as fluorescent labeling agents for immune serum. *Am. J. Pathol.* **34**, 1081–1097 (1958).
30. S. P. Amaral, M. Fernandez-Villamarin, J. Correa, R. Riguera, E. Fernandez-Megia, Efficient multigram synthesis of the repeating unit of gallic acid-triethylene glycol dendrimers. *Org. Lett.* **13**, 4522–4525 (2011).
31. J. S. Moore, S. I. Stupp, Room temperature polyesterification. *Macromolecules* **23**, 65–70 (1990).
32. R. Wong, S. J. Dolman, Isothiocyanates from tosyl chloride mediated decomposition of in situ generated dithiocarbamic acid salts. *J. Org. Chem.* **72**, 3969–3971 (2007).
33. D. Lingwood, K. Simons, Lipid rafts as a membrane-organizing principle. *Science* **327**, 46–50 (2010).
34. E. Sezgin, I. Levental, S. Mayor, C. Eggeling, The mystery of membrane organization: Composition, regulation and roles of lipid rafts. *Nat. Rev. Mol. Cell Biol.* **18**, 361–374 (2017).
35. C. Fastig *et al.*, Multivalency as a chemical organization and action principle. *Angew. Chem. Int. Ed. Engl.* **51**, 10472–10498 (2012).
36. E. Maria Munoz, J. Correa, R. Riguera, E. Fernandez-Megia, Real-time evaluation of binding mechanisms in multivalent interactions: A surface plasmon resonance kinetic approach. *J. Am. Chem. Soc.* **135**, 5966–5969 (2013).
37. L. L. Kiessling, M. B. Kraft, Chemistry. A path to complex carbohydrates. *Science* **341**, 357–358 (2013).
38. M. M. Sauer *et al.*, Binding of the bacterial adhesin FimH to its natural, multivalent high-mannose type glycan targets. *J. Am. Chem. Soc.* **141**, 936–944 (2019).
39. C. N. Scanlan, J. Offer, N. Zitzmann, R. A. Dwek, Exploiting the defensive sugars of HIV-1 for drug and vaccine design. *Nature* **446**, 1038–1045 (2007).
40. A. C. Walls *et al.*, Structure, function, and antigenicity of the SARS-CoV-2 spike glycoprotein. *Cell* **181**, 281–292.e6 (2020).
41. T.-J. Yang *et al.*, Cryo-EM analysis of a feline coronavirus spike protein reveals a unique structure and camouflaging glycans. *Proc. Natl. Acad. Sci. U.S.A.* **117**, 1438–1446 (2020).